

Multi-target quantum compilation algorithm

Vu Tuan Hai,^{1,*} Nguyen Tan Viet,² Jesus Urbaneja,³ Nguyen Vu Linh,^{4,5} Lan Nguyen Tran,^{4,5,†} and Le Bin Ho^{6,7,‡}

¹*Nara Institute of Science and Technology, Ikoma 630-0192, Nara, Japan*

²*FPT University, Hanoi, Vietnam*

³*Department of Mechanical and Aerospace Engineering, Tohoku University, Sendai 980-0845, Japan*

⁴*University of Science, Vietnam National University, Ho Chi Minh City 70000, Vietnam*

⁵*Vietnam National University, Ho Chi Minh City 70000, Vietnam*

⁶*Frontier Research Institute for Interdisciplinary Sciences, Tohoku University, Sendai 980-8578, Japan*

⁷*Department of Applied Physics, Graduate School of Engineering, Tohoku University, Sendai 980-8579, Japan*

(Dated: November 27, 2024)

Quantum compilation is the process of converting a target unitary operation into a trainable unitary represented by a quantum circuit. It has a wide range of applications, including gate optimization, quantum-assisted compiling, quantum state preparation, and quantum dynamic simulation. Traditional quantum compilation usually optimizes circuits for a single target. However, many quantum systems require simultaneous optimization of multiple targets, such as thermal state preparation, time-dependent dynamic simulation, and others. To address this, we develop a multi-target quantum compilation algorithm to improve the performance and flexibility of simulating multiple quantum systems. Our benchmarks and case studies demonstrate the effectiveness of the algorithm, highlighting the importance of multi-target optimization in advancing quantum computing. This work lays the groundwork for further development and evaluation of multi-target quantum compilation algorithms.

I. INTRODUCTION

Variational quantum algorithms (VQAs) like quantum approximate optimization algorithm (QAOA), variational quantum eigensolver (VQE), quantum neural networks (QNN), and quantum compilation (QC) are promising for solving practical tasks on noisy intermediate scale quantum (NISQ) devices beyond classical computers [1]. VQAs have proven to be versatile in various applications, including quantum state preparation [2–7], quantum dynamic simulation [7–10], and quantum metrology [11–15]. Recent developments underscore their ability to tackle complex quantum systems effectively.

In quantum state preparation, significant progress has led to various effective methods for generating target states with high fidelity [2–7]. For instance, Zhang et al. demonstrated that any quantum state can be prepared with a linear-depth circuit using many ancillary qubits, leading to exponential speedups for tasks like Hamiltonian simulation and solving linear systems [4]. Additionally, VQAs have been extensively studied for simulating quantum dynamics, employing adaptive variational principles to optimize the time evolution of quantum states [8]. This approach is particularly important for simulating open quantum systems, where the interaction between system dynamics and environmental factors plays a crucial role [16]. Furthermore, VQAs have demonstrated their capability to achieve quantum-enhanced precision in multiparameter quantum metrology, even in the presence of noise [14].

Quantum compilation, on the other hand, has gained significant interest due to its capacity to optimize quantum circuits through a training process that transforms target unitaries into trainable unitaries [17, 18]. This approach has been applied to various tasks, including gates optimization [17], quantum-assisted compiling [18], continuous-variable quantum learning [19], quantum state tomography [20], and quantum objects simulation [7]. For instance, a quantum object such as a quantum state can be prepared and its evolution can be simulated in a quantum circuit by using QC [7].

The performance of QCs relies on the number of qubits and the circuit depth. The choice of ansatzes (trainable quantum circuits) is also crucial and must be carefully selected. Some entangled topologies have shown promise in solving quantum state preparation problems but require many resources due to their numerous layers and parameters [6].

Traditional QCs focus on compiling a single target [7, 17–20] as mentioned above. However, many quantum systems require optimizing multiple factors at the same time, because independent optimization of each target can lead to suboptimal results in complex scenarios. For instance, simulating time-dependent quantum systems [8, 21–23] often requires balancing accuracy across various time intervals, while thermal-dependent systems [3, 24–26] demand simultaneous optimization of thermal fluctuations and quantum coherence to maintain system stability. Similarly, in multimode tomography [27, 28], optimizing multiple modes concurrently enhances the overall precision of quantum state estimation. These examples demonstrate that multi-target optimization is crucial in achieving optimal performance in quantum applications.

This work presents a multi-target quantum compila-

* Electronic address: vu.tuan_hai.vr7@naist.ac.jp

† Electronic address: tnlan@hcmus.edu.vn

‡ Electronic address: binho@fris.tohoku.ac.jp

tion algorithm to address these demands by providing a unified framework for optimizing multiple objectives simultaneously. Therein, we compile multiple unitaries into a single trainable unitary through an optimization process, improving the performance of QC and applicability in practical scenarios. We explain the theoretical foundations of our algorithm, its structure, and using techniques like the genetic algorithm (GA) to enhance the multi-target QC process. We show the effectiveness of our algorithm through benchmarking and case studies, including the preparation of thermal states and the simulation of time-dependent Hamiltonians in comparison with other methods including Trotterization [29, 30] and adaptive variational quantum dynamics simulations (AVQDS) [8]. We also provide a demonstration for the variational quantum eigensolver. The results highlight the importance of multi-target compilation in advancing quantum computing technologies and the potential for further innovation in this field.

The novelty of this work includes:

- It presents a quantum compilation algorithm for the first time that is adaptable for simulating multiple unitaries.
- It introduces an enhanced quantum architecture search that utilizes a genetic algorithm in combination with a standard variational quantum algorithm.

The paper is structured as follows. In Section II, we present the multi-target quantum compilation with detail of its definitions, algorithms, and numerical benchmarking. Section III explores various applications, including thermal state preparation, time-dependent quantum dynamic simulations, and variational quantum eigensolvers. Finally, we conclude the paper in Section IV. Additional material can be found in A and B.

II. MULTI-TARGET QUANTUM COMPILATION

Quantum compilation (QC) [6, 18] can be regarded as a training process that transforms information from a target unitary U to a trainable unitary $V(\boldsymbol{\theta})$, where $\boldsymbol{\theta}$ are trainable parameters. Hereafter, we introduce a compilation process to transform a set of n targets into one trainable unitary (one single quantum circuit with n different $\boldsymbol{\theta}$ s), therefore, it is called multi-target quantum compilation.

A. Definition

Let \mathcal{H} be a Hilbert space, and $\mathcal{U} = \{U_j; 1 \leq j \leq n\}$ be n -target unitaries on \mathcal{H} , there exists a trainable unitary V that satisfies

$$U_j V^\dagger(\boldsymbol{\theta}_j) = e^{-i\phi} \mathbb{I}, \quad \forall 1 \leq j \leq n, \quad (1)$$

where $\boldsymbol{\theta}_j \in \{\theta_j^{(1)}, \theta_j^{(2)}, \dots, \theta_j^{(m)}\}$ is a set of m trainable parameters and ϕ is a global phase. For each U_j , we need to maximize the kernel $\mathcal{K}_{U_j, V}(\boldsymbol{\theta}_j) = \frac{1}{u^2} |\text{Tr}[U_j V^\dagger(\boldsymbol{\theta}_j)]|^2$ where u is the dimension of U_j . For maximizing all $\mathcal{K}_{U_j, V}(\boldsymbol{\theta}_j), \forall U_j \in \mathcal{U}$, we define a cost function \mathcal{L} , which is the average infidelity

$$\mathcal{L}(\boldsymbol{\Theta}, V) = 1 - \frac{1}{n} \sum_{j=1}^n \mathcal{K}_{U_j, V}(\boldsymbol{\theta}_j), \quad (2)$$

where $\boldsymbol{\Theta} = (\boldsymbol{\theta}_1, \dots, \boldsymbol{\theta}_n)$ are trainable parameters, and $0 \leq \mathcal{L}(\boldsymbol{\Theta}, V) \leq 1$. The optimization process is to find $\boldsymbol{\Theta}^*, V^* = \text{argmin}_{\{\boldsymbol{\Theta}, V\}} \mathcal{L}(\boldsymbol{\Theta}, V)$. Here, we emphasize that not only the trainable parameters are optimized but also the structure of ansatz V is also optimized.

B. Quantum compilation algorithm

The training process in QC is a variational quantum algorithm (VQA). Given a target unitary U , it employs a gradient-based optimizer to update an ansatz $V(\boldsymbol{\theta})$ and find the optimal $\boldsymbol{\theta}^*$. The ansatz V is usually a multi-layer structure

$$V(\boldsymbol{\theta}) = \prod_{k=1}^L G_k(\boldsymbol{\theta}_k) \in \text{SU}(2^N), \quad (3)$$

where $G_k(\boldsymbol{\theta}_k)$ is a sequence of parameterized single- and multi-qubit quantum gates, L is the number of layers, N the number of qubits. The design of $V(\boldsymbol{\theta})$ is not unique, and recent efforts to optimize it, including architecture search [31–34], adaptive variational quantum algorithm [8, 35], and genetic-based approach (GA) [36–39].

In this work, we combine GA with VQA to optimize multi-target quantum compilation. This approach optimizes both the parameters and the structure of quantum circuits (ansatzes), ensuring efficient compilation, practical computational capability, and low-depth circuits. The scheme is shown in Figure 1(a), and the flow chart is given in Figure 1(b). We first generate quantum circuits with random parameters and evaluates their cost functions. If the cost functions do not meet a threshold, we use VQA to optimize the parameters and re-evaluate. After VQA finishes, the best circuits are passed to the GA, which updates their structure through selection, crossover, and mutation for the next generation. Once GA completes, the best circuit is fed back into the VQA, which runs until the threshold is met or the cost function stabilizes.

Concretely, denote the set of generated quantum circuits as $\mathcal{V} = \{V_l; 1 \leq l \leq n_V\}$, where n_V is the number of circuits. Each circuit $V_l \in \mathcal{V}$ is created from a pool of quantum gates. For each circuit V_l , we evaluate the average infidelity via $\mathcal{L}(\boldsymbol{\Theta}, V_l) \forall 1 \leq l \leq n_V$. If $\mathcal{L}(\boldsymbol{\Theta}, V_l) \leq \text{threshold}$, we designate V_l to the best circuit, $V^* \leftarrow V_l$, and $\boldsymbol{\Theta}$ will be the optimal parameters, $\boldsymbol{\Theta}^* \leftarrow \boldsymbol{\Theta}$. If not, we run the VQA scheme with gradient descent to update $\boldsymbol{\Theta}$ for a certain number of iterations

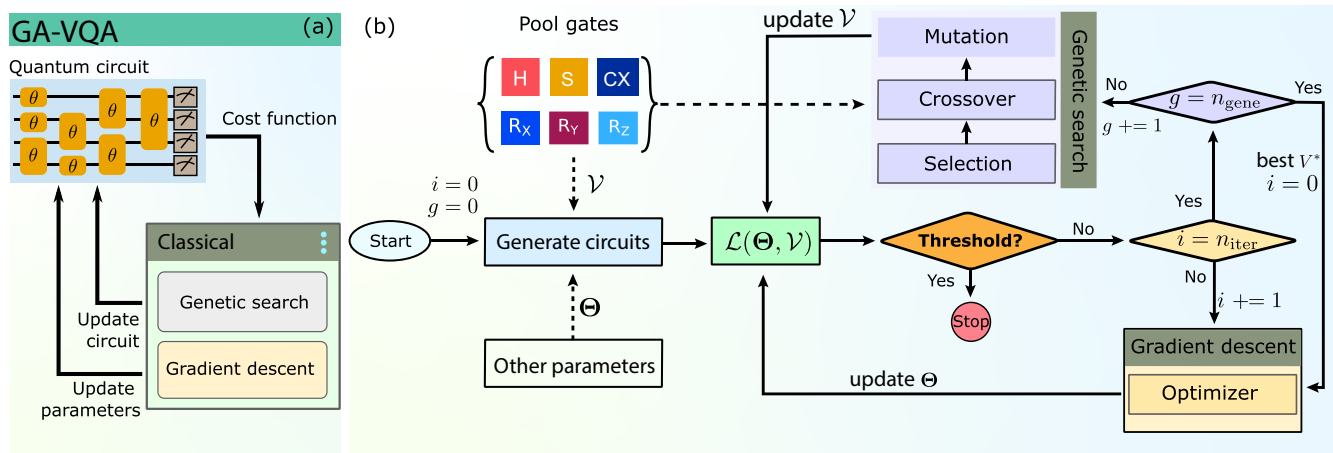


Figure 1. **Integrated Genetic Algorithm with Variational Quantum Algorithm (GA-VQA) for multi-target quantum compilation optimization.** (a) The GA-VQA method uses a parameterized quantum circuit and a classical computer to evaluate and update both the circuit structure and its parameters. (b) The process is as follows: (i) Generate a set of circuits \mathcal{V} and parameters Θ . (ii) Evaluate the cost function $\mathcal{L}(\Theta, V_l)$ for each circuit $l \in [1, n_{\mathcal{V}}]$. (iii) If the threshold is not met, use VQA followed by GA to find the best circuit, checking the threshold after each iteration. (iv) If the threshold is still not reached, pass the best circuit V^* back to VQA and repeat the process until the threshold is met. Here, i and g represent iteration indexes running up to n_{iter} and n_{gene} , respectively.

n_{iter} . Then, we use GA with selection, and mutation to create the next generation of \mathcal{V} . See A for a detailed evolution of the GA. The GA scheme repeats until the threshold is met or the number of generations n_{gene} is reached. Finally, if n_{gene} is reached without meeting the threshold, we pass the best circuit V^* to the VQA scheme again, and optimize Θ until the threshold is met.

In this framework, we run the VQA process twice. The first run aims to create a suitable $\mathcal{L}(\Theta, V_l)$ for evaluating the GA evolution process. We can choose a small n_{iter} in this step to reduce computational cost. The second run occurs after the GA and aims to optimize Θ to ensure that $\mathcal{L}(\Theta^*, V^*)$ is minimized within the best circuit V^* .

Our scheme differs from the one-stage [31] and two-stage architecture search [33, 40]. In those methods, all circuits are generated, their cost functions are evaluated as the low-depth and high number of gates as much as possible (gate density [41] close to unity), and they are sorted from best to worst to select the top one. In our approach, each circuit $V_l \in \mathcal{V}$ is evaluated and compared with the best circuit (initially set as V_1). We thus do not require space to store all circuits. Although genetic algorithms have been suggested for quantum state tomography [42], we believe they are also promising for different types of VQAs, including our proposed method for quantum compilation.

So far, we have observed that Ashhab et al. found that if a quantum circuit can perfectly implement one arbitrary target using random search, it can also implement any other targets with the same gate configuration. It only requires recalculating the single-qubit rotation parameters for each new target [43, 44]. This finding is similar to our discovery here using quantum compilation.

C. Numerical illustration

For numerical evaluation, we follow Ref. [45] and divide a random set \mathcal{U} into a training set $\mathcal{U}_{\text{train}} = \{U_1, U_2, \dots, U_{\text{train}}\}$ and a testing set $\mathcal{U}_{\text{test}} = \{U_{\text{train}+1}, U_{\text{train}+2}, \dots, U_n\}$. We then train the model on $\mathcal{U}_{\text{train}}$ using the cost function $\mathcal{L}(\Theta_{\text{train}}, V_l)$ as in Eq. 2. After training, we get the best circuit V^* and evaluate the expected risk \mathcal{R} over $\mathcal{U}_{\text{test}}$

$$\mathcal{R}(\Theta_{\text{test}}) = \frac{1}{4} \mathbb{E}_{U_j \in \mathcal{U}_{\text{test}}} \left\| U_j |\mathbf{0}\rangle \langle \mathbf{0}| U_j^\dagger - [V^*]^\dagger (\theta_j) |\mathbf{0}\rangle \langle \mathbf{0}| V^*(\theta_j) \right\|_1^2, \quad (4)$$

where $|\mathbf{0}\rangle \equiv |0\rangle^{\otimes N}$, with N is the number of qubits.

Figure 2(a-d) shows the correlation between risk \mathcal{R} and fidelity $\mathcal{F} = 1 - \mathcal{L}$ for several n_{gene} and $n_{\mathcal{V}}$ with $N = 3$. The GA-VQA method identifies a low-risk, high-fidelity ansatz for multi-target Haar random unitaries. Additionally, the factors n_{gene} and $n_{\mathcal{V}}$ have minimal impact on the results, allowing GA-VQA to run efficiently with minimal values, thus saving computational resources. The variation in some cases, such as the yellow lines in Figure 2(a-c), is a result of fluctuations in the optimization process for specific parameter settings. These fluctuations can arise from the randomized nature of the initial population in the genetic algorithm or the stochastic behavior of the variational quantum algorithm (VQA). Furthermore, the performance of different circuit architectures can vary significantly, leading to occasional deviations in the optimization trajectory.

Figure 2(e) shows fidelity versus depth d for 2-5 qubits. As expected, higher N requires larger d to achieve high

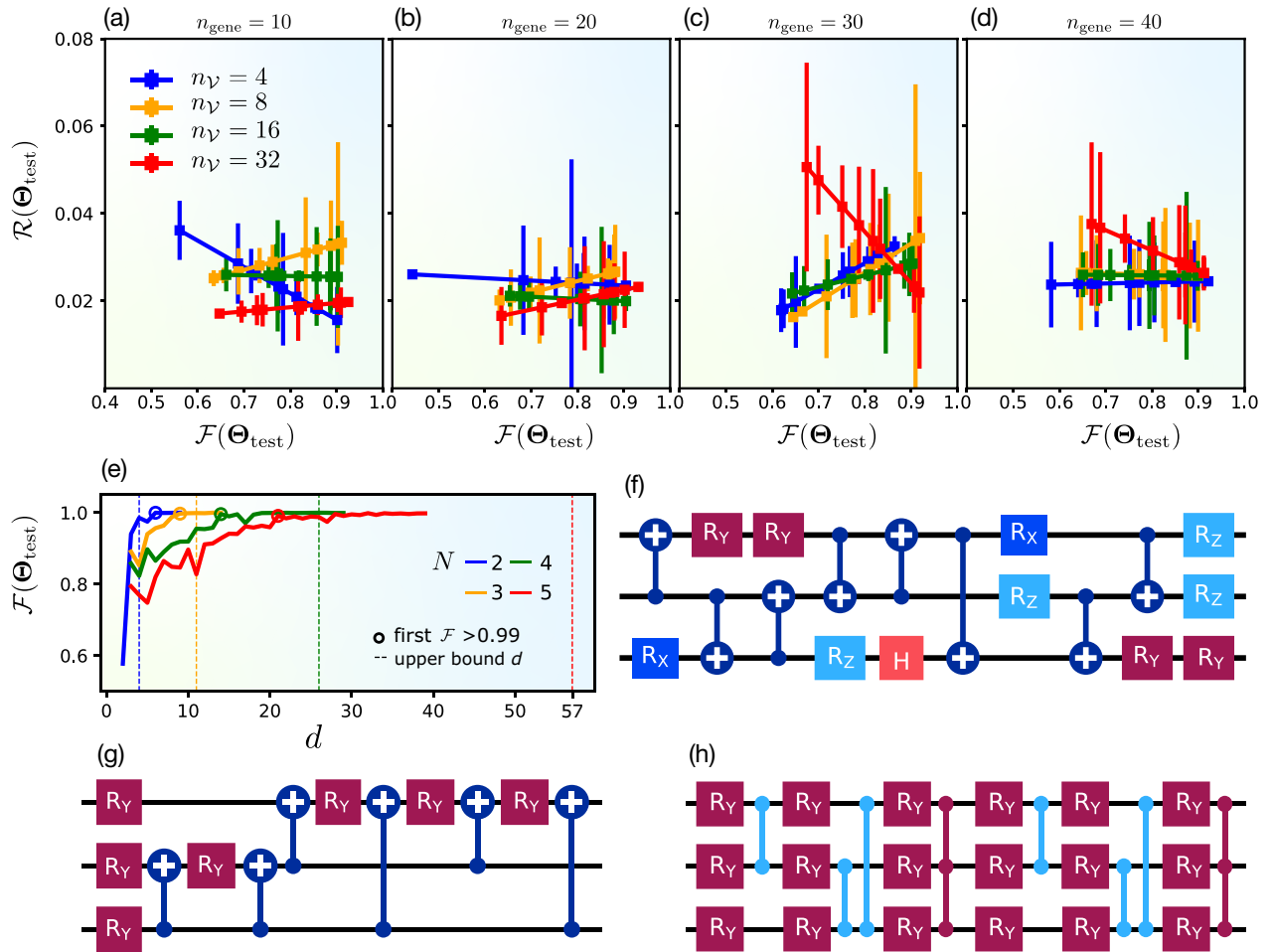


Figure 2. **Numerical benchmarking for a set of Haar random \mathcal{U} .** (a-d) Correlation between risk and fidelity for different number of generations n_{gene} and circuits per generation $n_{\mathcal{V}}$. (e) Plot of fidelity versus depth d for different number of qubits N ranging from 2 to 5. (f) The best quantum circuit generated by GA-VQA for $N = 3$ with $d = 9$. (g) The quantum circuit generated by Qiskit with $d = 11$. (h) $|g_{2g_N}\rangle$ (2 layers) ansatz before transforming into single and two-qubit gates.

fidelity. In the figure, circles mark the depth where $\mathcal{F} \geq 0.99$, with upper bounds generated by the standard Qiskit method. Figure 2(f) shows the best circuit generated by our GA-VQA compared to the Qiskit-generated circuit in Figure 2(g) and the $|g_{2g_N}\rangle$ ansatz[6] in Figure 2(h) for $N = 3$. The GA-VQA circuit has the shortest depth (9), compared to 11 and 38 for the others. Table I shows detailed comparisons for 2 to 5 qubits, demonstrating that the GA-VQA circuit provides high fidelity with the smallest depth.

Table I. Comparison between three methods: GA-VQA, default Qiskit preparation, and $|g_{2g_N}\rangle$ (2 layers). All circuits are transpiled with the same gate set $\{H, S, CX, R_i(\theta)\}$ with $i \in \{x, y, z\}$.

N	\mathcal{F}	Depth (d)	#gates (#1-qubit gate + #2-qubit gate)		#parameters	
2	0.92	3	GA-VQA	Qiskit	GA-VQA	Qiskit
3	0.99	9	GA-VQA	Qiskit	GA-VQA	Qiskit
4	0.99	15	GA-VQA	Qiskit	GA-VQA	Qiskit
5	0.99	27	GA-VQA	Qiskit	GA-VQA	Qiskit

^{*}The number of parameters in GA-VQA differ for each run depending on the set of gates in the best circuit.

D. The complexity of GA-VQA

We discuss here the complexity of GA-VQA. Time complexity describes how the runtime of an algorithm changes as the input size increases, usually expressed using Big-O notation. It gives an estimate of the maximum runtime as the input grows. Common complexities include $\mathcal{O}(1)$ for constant time, $\mathcal{O}(z)$ for linear time, $\mathcal{O}(z^2)$ for quadratic time, and $\mathcal{O}(\log z)$ for logarithmic time. Here, z is the input size. The time complexity of GA-VQA is defined as $\mathcal{O}(n \times n_{\text{gene}} \times n_{\mathcal{V}} \times \mathcal{F})$ which depends on the number of targets n , the number of generations n_{gene} , the number of circuits in each generation $n_{\mathcal{V}}$, and the fidelity \mathcal{F} . When the fidelity of circuits in one generation can be evaluated concurrent (parallel mode), the actual time complexity is $\mathcal{O}(n_{\text{gene}} \times n_{\mathcal{V}} \times \mathcal{F})$, assuming that number of processing cores is larger than n .

The space complexity of an algorithm refers to the amount of memory or storage it requires relative to the size of the input. The space complexity in our case is

$O(n \times n_{\mathcal{V}} \times \mathcal{F})$.

Since $n_{\text{gene}}, n_{\mathcal{V}}$ are hyper-parameters, the time and space complexities heavily depend on the cost function. For instance, for GA-VQA applied to multi-target compilation, the time complexity is approximately $\mathcal{O}(n_{\text{gene}} \times n_{\mathcal{V}} \times n_{\text{iter}} \times 2^N \times d)$, where d is the circuit depth and n_{iter} is the number of optimization iterations. The space complexity for a state vector simulator is at least $\mathcal{O}(n \times n_{\mathcal{V}} \times 2^N)$. For example, with 8 GB of RAM, GA-VQA can support up to 10 qubits with $n = 5$ and $n_{\mathcal{V}} = 4$, which results in approximately 6 GB used, calculated as follows: 5×4 (for concurrent processes), $64 \times 2 \times (2^{10} + 2^{20})$ (for a double-precision, 10-qubit quantum state-operator), multiplied by 2 for each buffer (state and circuit).

Currently, GA-VQA can manage unitaries that act on around 8-10 qubits with moderate circuit depths of approximately 40. More details can be found in B. However, this estimate may change with advancements in hardware capabilities, such as improved qubit coherence times and error rates. These factors are also the bottleneck for scaling the system size.

III. APPLICATIONS

A. Thermal state preparation (TSP)

Quantum state preparation using quantum algorithms is well-studied for pure states [2, 5, 6]. However, preparing mixed states requires purification first, followed by the preparation of the pure state [46]. The conventional purification method needs $2N$ qubits to prepare a mixed state of N qubits. Here, we propose a ‘‘dense-purification’’ method that needs only N qubits.

A quantum state ρ in a u -dimensional Hilbert space \mathcal{H}_A can be represented using its eigenvalues and eigenstates as $\rho = \sum_{j=1}^u p_j |j\rangle\langle j|$. In conventional purification, we create a pure state $|\psi\rangle$ in a larger Hilbert space $\mathcal{H}_A \otimes \mathcal{H}_B$, where \mathcal{H}_B is another u -dimensional Hilbert space with an orthonormal basis $\{|j\rangle_B\}$. The pure state is $|\psi\rangle = \sum_j \sqrt{p_j} |j\rangle_A |j\rangle_B$, purifying ρ such that $\rho = \text{Tr}_B[|\psi\rangle\langle\psi|]$. In our dense-purification method, we define a pure state $|\psi\rangle = \sum_j \sqrt{p_j} |j\rangle$, directly representing the dense-purified state of ρ . It can be shown that $\rho = \text{diag}(|\psi\rangle\langle\psi|)$, allowing us to extract various properties of ρ from $|\psi\rangle$.

We demonstrate the preparation of thermal equilibrium states, specifically Gibbs states at fixed temperatures. These states are crucial for various applications, such as quantum simulation [47], quantum machine learning [48], quantum condensed matter [49], quantum field theory [50], and cosmology [51, 52]. We focus on the Gibbs state of a transverse field Ising model (TFIM) [53], which is useful for studying thermal phase transitions in condensed matter physics.

In the TFIM model on a ring of N sites, the Hamiltonian takes the form $H = \sum_{i=1}^N Z_i Z_{i+1} + \sum_{i=1}^N X_i$, where

X and Z are Pauli matrices. In this model, the Gibbs state is defined as $\rho(\beta) = e^{-\beta H}/Z(\beta)$ where $\beta = k_B T$ is the inverse temperature and $Z(\beta) = \text{Tr}[e^{-\beta H}]$ is the partition function. At $\beta = 0$, the Gibbs state is maximally mixed, and it gradually becomes a pure state when $\beta \rightarrow \infty$.

Conventionally, to prepare this mixed state on a quantum computer, previous approaches used the conventional purification scheme as [3, 24–26]

$$|\psi(\beta)\rangle = \frac{1}{\sqrt{Z(\beta)}} \sum_j e^{-\beta E_j/2} |j\rangle_A |j\rangle_B, \quad (5)$$

where $Z(\beta) = \sum_j e^{-\beta E_j}$. Here, E_j and $|j\rangle$ are the eigenvalues and eigenstates of H , i.e., $H|j\rangle = E_j|j\rangle$. The purified state is known as thermofield double (TFD) state [3], which related to the Gibbs state through $\rho(\beta) = \text{Tr}_B[|\psi(\beta)\rangle\langle\psi(\beta)|]$.

For the dense-purification approach, the dense-purified state is given by

$$|\psi_{\text{dense}}(\beta)\rangle = \frac{1}{\sqrt{Z(\beta)}} \sum_j e^{-\beta E_j/2} |j\rangle_A. \quad (6)$$

Previously, QAOA [3, 24, 25, 54] and parametrized circuits [26] were used to prepare the quantum state in (5). Here, we apply our GA-VQA to prepare the states in Eqs. (5, 6). We evaluate the closeness of the prepared state to the target state using fidelity and purity metrics

$$\mathcal{F} = \text{Tr} \left[\sqrt{\sqrt{\rho(\beta)} \check{\rho}(\beta) \sqrt{\rho(\beta)}} \right]^2; \quad \text{and } \mathcal{P} = \text{Tr}[\check{\rho}(\beta)], \quad (7)$$

where $\check{\rho}(\beta) = \text{Tr}[|\psi(\beta)\rangle\langle\psi(\beta)|]$ for conventional purification and $\check{\rho}(\beta) = \text{diag}[|\psi_{\text{dense}}(\beta)\rangle\langle\psi_{\text{dense}}(\beta)|]$ for dense purification. See B for details on preparing $|\psi(\beta)\rangle$ and $|\psi_{\text{dense}}(\beta)\rangle$.

In Figure 3(a), we set $N = 2$ and examine \mathcal{F} and \mathcal{P} while comparing them in different methods. We demonstrate that both methods align well with the theory, proving the efficacy of the preparation method for creating Gibbs states. In Figure 3(b), we show the corresponding quantum circuits, where the dense method requires fewer qubits and lower circuit depth compared to the conventional method. Next, we focus on the dense method with $\beta = 2$. Figure 3(c) shows the fidelity versus the number of qubits N with the results closely approaching one (theory) for all N , and the square error is on the order of 10^{-5} as depicted in Figure 3(d). Similarly, we analyze the purity and its error in Figure 3(e,f), which align well with the theory.

B. Time-dependent quantum dynamic simulation (TD-QDS)

In this section, we demonstrate for dynamic time-dependent simulations. We consider a one-dimensional

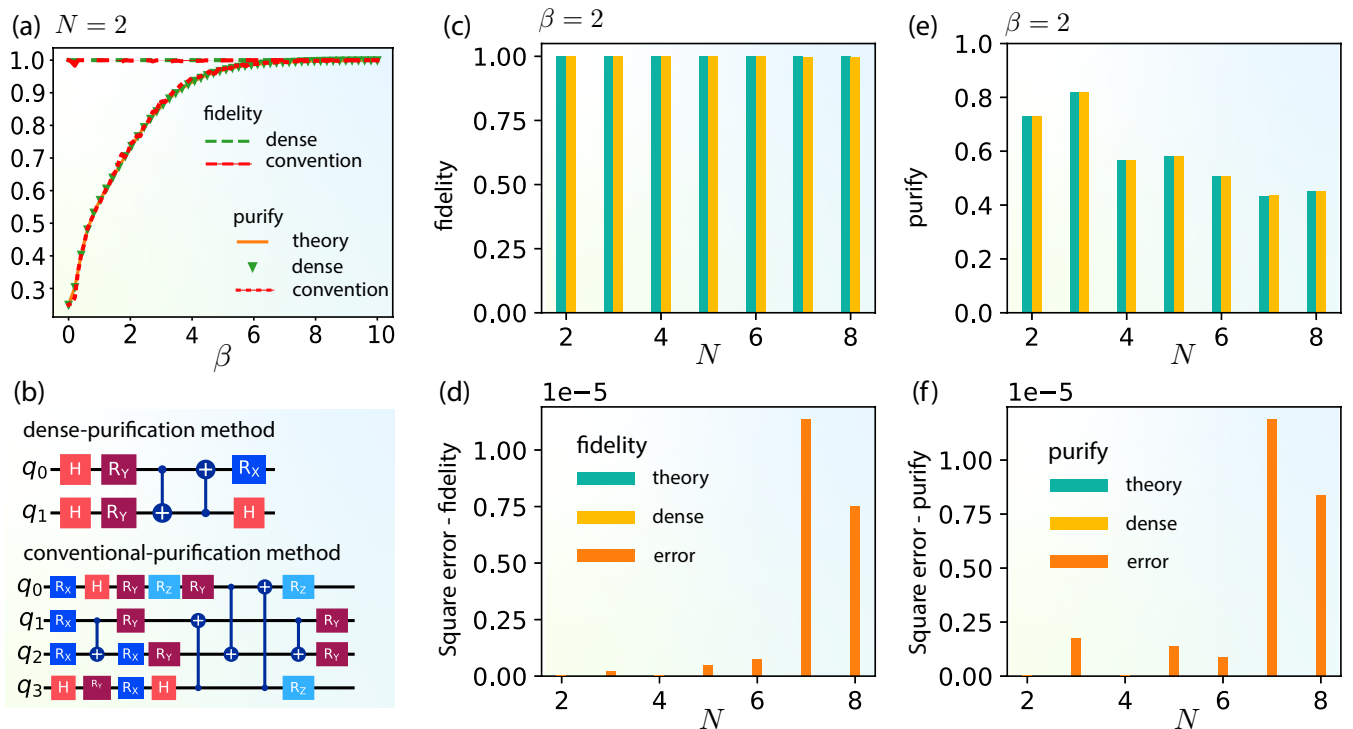


Figure 3. **Thermal states preparation.** (a) Comparison of fidelity and purity versus β at $N = 2$ for various methods, alongside theoretical predictions. (b) Quantum circuits used in dense and conventional methods. (c) Fidelity plotted against N at $\beta = 2$. (d) Square error of fidelity plotted against N at $\beta = 2$. (e) Purity plotted against N at $\beta = 2$. (f) Square error of purity plotted against N at $\beta = 2$. The legends for (c) and (e) are the same as (d) and (f).

spin-1/2 system with N spins, initially prepared in a do-

main wall configuration $|\psi_0\rangle = |\cdots \downarrow\uparrow\uparrow\cdots\rangle$. The time-dependent Hamiltonian is given by

$$H(t) = -\frac{J}{2} \sum_{j=1}^{N-1} \left[\left(1 - \frac{t}{T}\right) X_j X_{j+1} + \left(1 + \frac{t}{T}\right) Y_j Y_{j+1} \right] + u \sum_{j=1}^{N-1} Z_j Z_{j+1} + h \sum_{j=1}^N X_j, \quad (8)$$

where J and u are coupling strengths, h is the external magnetic field, and X, Y, Z are Pauli matrices. The evolution is given by

$$U(t) = \mathcal{T} \exp \left(-i \int_0^t ds H(s) \right), \quad (9)$$

where \mathcal{T} is the time-ordering operator, and $\hbar = 1$ is used throughout the paper. We consider the local magnetization as the dynamical quantity to be examined

$$M_j(t) = \langle \psi(t) | Z_j | \psi(t) \rangle, \quad (10)$$

where $|\psi(t)\rangle$ is the quantum state given at time t .

The local magnetization is shown in Figure 4, comparing the exact result with various methods, including GA-VQA, Trotterization [29, 30] with first order (Trotter1) and second order (Trotter2), and adaptive variational quantum dynamics simulations (AVQDS) [8]. We

set $N = 2, J = 1, T = 10$ and consider several models for u and h as shown in the figure. For the theoretical computation, the local magnetization is given by Eq. (10), with the final state directly computed from $U(t)$ yielding $|\psi(t)\rangle = U(t)|\psi_0\rangle$. For the other simulation methods, the local magnetization is derived from the measured probabilities of the final circuit. See detailed calculation in B.

The GA-VQA results closely match the exact results over time for all models, demonstrating the method's reliability and versatility in capturing quantum dynamics. Trotter2 also achieves high accuracy, aligning well with exact results in cases (a) and (b), but shows deviations in case (c). Trotter1 and AVQDS match well with theoretical predictions only in case (a) and deviate as time t increases in cases (b) and (c). Deviations in Trotter1 are common, as noted in previous studies [29, 30, 55], while

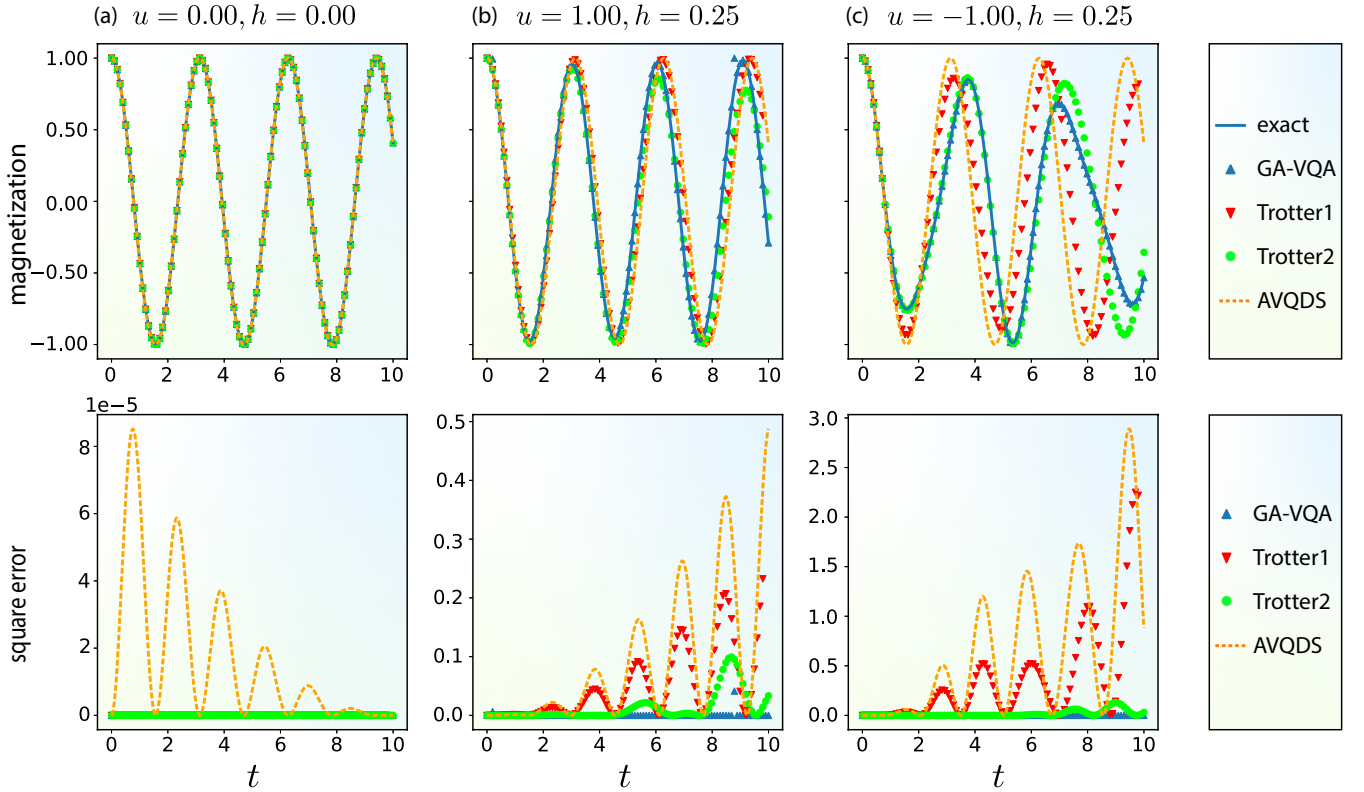


Figure 4. **Time-dependent quantum dynamic simulation.** Plot of the local magnetization versus time (upper) and its square error (lower) for several models: (a) $u = 0.00, h = 0.00$, (b) $u = 1.00, h = 0.25$, (c) $u = -1.00, h = 0.25$. Here we set $N = 2, J = 1$ and $T = 10$. We compare various methods with the theory, including GA-VQA, Trotter1, Trotter2, and AVQDS.

discrepancies in AVQDS results stem from simplifications in our calculations, as discussed in B.

C. Demo application for Variational Quantum Eigensolver (VQE)

In this section, we extend the proposed multi-target compilation approach into VQE. It is a quantum algorithm used to estimate the lowest eigenvalue of a given Hamiltonian, which is crucial in quantum chemistry and optimization problems. It employs a parameterized quantum circuit to prepare trial states and a classical optimization routine to adjust these parameters iteratively, converging towards the lowest eigenvalue. This algorithm is handy in problems where the direct calculation of eigenvalues is computationally expensive, making it a promising candidate for near-term quantum computer applications.

The unitary coupled cluster with singles and doubles (UCCSD) ansatz was used in the first proposal of the VQE algorithm [56]. While achieving high accuracy and attracting significant research interest, the UCCSD ansatz requires a large number of gates and a high depth [57], due to their “staircase” structure. This makes it less suitable for the Noisy Intermediate-Scale Quantum

(NISQ) era.

Here, we apply the developed GA-VQA to find a more efficient ansatz for electronic structure ansatz. For this purpose, we use the cost function as the energy

$$\mathcal{L}_{\text{VQE}}(\Theta, V_l) = \sum_{j=1}^n \langle \mathbf{0} | V_l^\dagger(\theta_j) H_j V_l(\theta_j) | \mathbf{0} \rangle; \forall l \leq n_V, \quad (11)$$

where $|\mathbf{0}\rangle \equiv |0\rangle^{\otimes N}$ is a reference state, $H_j \in \mathcal{H} \forall j = \{1, \dots, n\}$ is a set of n target Hamiltonians with respect to the molecular distances $R = \{R_1, R_2, \dots, R_n\}$, and V_l is a quantum circuit found by the GA-VQA scheme.

We apply the GA-VQA scheme to the Hydrogen molecule. In Figure 5(a), we estimate the ground state potential energy surface by optimizing VQE with the best ansatz from the GA-VQA method for ten points ($n = 10$), achieving accuracy comparable to the UCCSD ansatz. Here, we approximate the UCCSD ansatz with only the first-order Suzuki-Trotter approximation. Figure 5(b) shows the convergence of fidelity versus n_{gene} for $d = 15, 18, 20, 24$, and 25 , with their best fidelities plotted in Figure 5(c). As seen in Figure 5(d), the ansatzes identified by GA-VQA possess more parameters compared to UCCSD ansatz but require significantly less depth. Even with the first-order Trotter decomposition, the UCCSD ansatz demands a depth of 74. Conse-

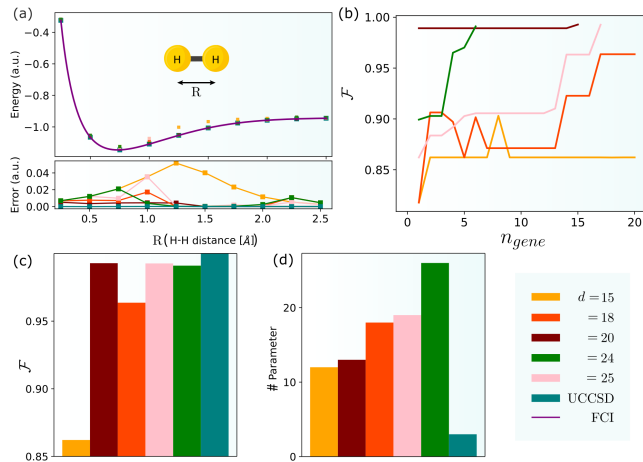


Figure 5. **The application of GA-VQA scheme to Variational Quantum Eigensolver Algorithm for Hydrogen molecule** (a) Comparison of UCCSD ansatz and GA-VQA found ansatz in estimating ground state energy surface of the Hydrogen molecule. (b) The fidelity for different depth GA-VQA found ansatz as a function of optimization step n_{gene} . (c) The best fidelity of GA-VQA found and UCCSD ansatz. (d) The number of parameters in GA-VQA found and UCCSD ansatz.

quently, the GA-VQA found ansatzes are more suitable for the NISQ era. Details on the technical methods used in these findings are provided in B.

IV. CONCLUSION

We introduced a novel multi-target quantum compilation algorithm aimed at optimizing quantum circuits for multiple objectives simultaneously. By leveraging a genetic algorithm (GA) combined with variational quantum algorithms (VQAs), we were able to efficiently optimize both the structure and parameters of quantum circuits. Our benchmarks and case studies demonstrated the algorithm’s capability to outperform traditional approaches, particularly in scenarios requiring simultaneous optimization, such as simulating thermal states and time-dependent systems. This method offers a significant advancement in quantum compilation, providing a foundation for further exploration in multi-target optimization and its potential applications in quantum computing.

Although this work focuses on developing the multi-target quantum compilation algorithm, analyzing its performance in noisy environments, especially on NISQ devices, is crucial. Noise can affect both the convergence of the genetic algorithm and the fidelity of the compiled circuits. In future works, we will include noise models to assess the algorithm’s robustness and explore strategies to mitigate noise, enhancing convergence and maintaining high fidelity.

ACKNOWLEDGMENTS

L.B.H. thanks Dr. Sahel Ashhab for the fruitful discussions. V.T.H. expresses gratitude to Dr. Luong Ngoc Hoang for advice on genetic algorithms. This research is funded by JSPS KAKENHI Grant Number 23K13025, Unitary Fund, and Tohoku University FRIS URO. L.N.T is partially supported by Vietnam National University Ho Chi Minh City (VNU-HCM) under grant number C2024-28-04.

DATA AVAILABILITY

Data are available from the corresponding authors upon reasonable request.

CODE AVAILABILITY

The code is available at <https://github.com/vutuanhai237/GA-QAS>.

AUTHOR CONTRIBUTIONS STATEMENT

V.T.H. wrote the GA-QAS code and conducted the numerical simulation. N.T.V. and J.U. implemented the thermal state preparation. J.U. and L.B.H. carried out the time-dependent dynamics simulation. N.V.L. implemented the VQE demo. L.N.T proposed and supervised the VQE demo. L.B.H. proposed the theory of multi-target quantum compilation and supervised its application to thermal state preparation and time-dependent dynamics simulation. L.N.T and L.B.H. supervised the entire project. All authors discussed the results and contributed to writing the manuscript.

COMPETING INTERESTS

The author declares no competing interests.

Appendix A: Structure of GA

1. GA scheme

First, let us define some terminologies used in common genetic science and their counterpart in quantum circuits. These terminologies are given in Tab. II below.

In a GA scheme, each quantum circuit (individual gene) will be randomly generated from a pool gate with a fixed circuit depth, which consists of various types of quantum gates with one qubit, two qubits, to one-parameter, and two-parameter. The more gates used, the more possible candidates. This increases the likelihood of

Table II. List of terminologies used in the common genetic science and their counterpart in quantum circuits.

Genetic science		Quantum circuit	
Name	Description	Name	Description
1 DNA/RNA	genetic material	quantum gate	unitary operator
2 individual	genetic unit	quantum circuit	a set of quantum gates
3 population	a group of genes	a set of quantum circuits	a set of quantum circuits
4 fitness	performance metric	cost function	performance metric

finding a suitable candidate but at the same time expands the search space, making us spend more time. Furthermore, using basic gates such as Clifford set = $\{H, S, CX\}$ [58] enables to implementation of candidates in a real quantum computer, two-qubit gates will be used restrictively. In general, our pool is $\{H, S, CX, R_i(\cdot)\}$ with $i \in \{x, y, z\}$. Although the H and S gates can be expressed using $R_i(\cdot)$, they are essential for reducing the complexity of the ansatz, including lowering the number of parameters and minimizing circuit depth.

The scheme will produce a set of quantum circuits and evaluate their fitness using a fitness function to identify the optimal quantum circuit. If the best fitness falls short of a predetermined threshold, an evolutionary process involving selection, crossover, and mutation will be implemented to generate a new circuit. This process will be repeated iteratively until the threshold is met or till the end number of generation, we then switch to VQA to optimize parameters Θ .

2. Selection-Crossover-Mutation

There are many types of selection, crossover, and mutation functions:

- Selection: Tournament, Proportional, Rank, Elitist,...
- Crossover: One-point, N-point, Uniform, Linear combination,...
- Mutation: Random deviation, Exchange, Shift, Bit flip, Inversion, Shuffle,...

In this work, we used Elitist Selection, One-point Crossover, and Bit Flip Mutation as the default option. We plan to investigate other combinations in future studies. After generating a set of quantum circuits \mathcal{V} , we evaluate them using cost functions like fidelity and retain only the two best candidates as elitist circuits for the next generation. These selected candidates are paired for crossover to create new ones. Each pair of parents (p_1, p_2) is divided into four parts $\{p_{11}, p_{12}, p_{21}, p_{22}\}$ at one point, normally center point. Two new candidates (c_1, c_2) are formed by combining these parts: $c_1 = \{p_{11}, p_{22}\}$ and $c_2 = \{p_{21}, p_{12}\}$. In each generation, there is a small probability (1%) that any gate (bit) in a candidate will mutate and be replaced (flip) with a different gate from the pool.

Appendix B: Detailed experimental setting

All numerical findings are implemented in Python using Qiskit 0.45.1 with QASMSimulatorPy simulation to verify algorithm convergence. We benchmark 2 to 10 qubits on several computer systems, including 24 nodes CPU Intel Xeon X5675 High-performance computer (HPC) at Vietnam Academy Science & Technology, Intel X299-GPU A6000 Workstation and AMD EPYC 7713P cluster at Tohoku University, and Intel Core i9-10940X CPU at NAIST, Japan.

We mainly use gradient-based method with Adam optimizer (except for the VQE), where a set of θ is updated through

$$\theta^{k+1} = \theta^k - \alpha \frac{\hat{m}_k}{\sqrt{\hat{v}_k + \epsilon}}, \quad (\text{B.1})$$

where $m_k = \beta_1 m_{k-1} + (1 - \beta_1) \nabla_{\theta} \mathcal{L}(\theta)$, $v_k = \beta_2 v_{k-1} + (1 - \beta_2) \nabla_{\theta}^2 \mathcal{L}(\theta)$, $\hat{m}_k = m_k / (1 - \beta_1^k)$, $\hat{v}_k = v_k / (1 - \beta_2^k)$, with the hyper-parameters are chosen as $\alpha = 0.2$, $\beta_1 = 0.8$, $\beta_2 = 0.999$ and $\epsilon = 10^{-8}$. The gradient $\partial_{\theta} \mathcal{L}(\theta)$ is given through the general parameter-shift rule [59].

1. Numerical benchmarking

For numerical benchmarking, we generated Haar random unitaries, using 20 for training and 10 for testing at each time. We ran GA-VQA on the training set with:

- $n_{\text{iter}} = 100$,
- threshold = 0.01,
- n_{gene} ranging from 10 to 40,
- $n_{\nu} = [4, 8, 16, 32]$,
- Depth d from 2 to 39,

and get the best circuits for each setup. We use these best circuits to calculate the risk on the testing set. All results in Figure 2 are for the testing set.

2. Thermal state preparation

a. Conventional purification method.

For the conventional purification method, we examine for $N = 2$ thermal state, which requires a 4-qubit circuit.

Initially, we generate 100 target TFD states corresponding to equally-spaced $\beta \in [0, 10]$. We then run GA-VQA to find the best circuit structure for all those TFD states based on the weighted-sum cost function as we will explain below. Finally, we continue to run optimization using Adam optimizer for 100 iterations to find optimal parameters for each quantum state.

The circuit depth is 29 after transpiling. Other configurations include $n_{\text{iter}} = 100$, $n_{\mathcal{V}} = 16$, $n_{\text{gene}} = 20$. Furthermore, optimal parameters with $\beta < 1$ are harder to find than those with $\beta > 1$. A simple average of cost values in the interval β from 0 to 10 is not sufficient for finding near-optimal ansatzes in the range β from 0 to 1. To address this, we use a weighted average cost function for different intervals. Specifically, we assign weights $w_1 = 2.2, w_2 = 1.6, w_3 = 0.9$ to three corresponding intervals $\beta \in [0, 4), \beta \in [4, 7)$, and $\beta \in [7, 10]$. The weighted-sum cost function is expressed as

$$\mathcal{F}_{\text{ws}} = \frac{w_1 * \mathcal{F}_{\beta \in [0,4)} + w_2 * \mathcal{F}_{\beta \in [4,7)} + w_3 * \mathcal{F}_{\beta \in [7,10]}}{w_1 + w_2 + w_3}, \quad (\text{B.2})$$

where $\mathcal{F}_{\beta \in [i,j)}, 0 \leq i, j \leq 10$ is the average fidelity in the interval $[i, j)$.

b. Dense-purification method.

We examine thermal state preparation using the dense-purification method across 2 to 8 qubits. Parameters include $n_{\text{iter}} = 100$, $d = 2N$, $n_{\mathcal{V}} = 8$, $n_{\text{gene}} = 16$. Note that n_{gene} does not significantly affect the runtime, as the program can stop anytime if the threshold is met. The threshold and optimizer remain consistent with the

previous settings. Note that in this case, the cost function is fidelity \mathcal{F} in Eq. (7).

3. Time-dependent dynamic simulation

a. GA-VQA method.

For the GA-VQA method, our simulation follows these steps: (1) Create the initial state $|\psi_0\rangle = |11\dots 00\rangle$ by applying X gates to $N/2$ qubits. (2) Create a set of 100 target unitaries $U(t_i)$ using Eq. (9) for $t_i \in [0, 10]$, $i = \{1, 2, \dots, 100\}$. (3) We then run GA-VQA to find the best circuit structure for all those target unitaries. Once $V^*(\Theta^*)$ is determined, we measure the magnetization as follows. (i) Prepare $|\psi_0\rangle$ in a quantum circuit. (ii) Apply $V^*(\Theta^*)$ to get the final state $|\check{\psi}(t)\rangle = V^*(\Theta^*)|\psi_0\rangle$. (iii) Measure qubit j and get the probability

$$p_j(m) = \langle \check{\psi}(t) | \Pi_j | \check{\psi}(t) \rangle, \text{ for } m \in \{0, 1\}, \quad (\text{B.3})$$

where $\Pi_j = I_1 \otimes \dots \otimes |m_j\rangle\langle m_j| \otimes \dots \otimes I_N$. Finally, the local magnetization (10) is given by

$$M_j(t) = p_j(0) - p_j(1). \quad (\text{B.4})$$

We benchmark for 2-qubit case. The parameters used for this case include: $n_{\text{iter}} = 500$, $d = 4$, $n_{\mathcal{V}} = 8$, $n_{\text{gene}} = 16$, and the local magnetization was taken for the second qubit. See Tab. III for a summary.

b. Trotterization method.

To implement the Trotterization, we break down the evolution $U(t_i)$ as follows

$$U(t_i) = \exp \left[-i \int_{t_{i-1}}^{t_i} H(s) ds \right] \\ = \exp \left\{ -i \frac{\delta t}{K} \lim_{K \rightarrow \infty} \left[H(t_{i-1}) + H(t_{i-1} + \frac{\delta t}{K}) + \dots + H(t_{i-1} + \frac{(K-1)\delta t}{K}) \right] \right\}, \quad (\text{B.5})$$

where $\delta t = t_i - t_{i-1} = 0.1$ is the interval, divided into K equal sub-intervals. Here, we set $K = 5$, making $\delta t/K = 0.02$ sufficiently small. Each $H(s)$ in the above expression consists of single and two-qubit gates, and we assume $H(s) = \sum_{j=1}^L H_j$. Using Trotterization, we can

break $H(s)$ own into a sequence of quantum gates and implement it in quantum circuits. The Trotterization expansions of the first order (Trotter1) and second order (Trotter2) are given by [30, 60]

$$e^{-iH(s)} = \lim_{r \rightarrow \infty} \left(e^{-i\frac{H_L}{r}} \dots e^{-i\frac{H_1}{r}} \right)^r \text{ for Trotter1, and} \quad (\text{B.6})$$

$$e^{-iH(s)} = \lim_{r \rightarrow \infty} \left[\left(e^{-i\frac{H_L}{2r}} \dots e^{-i\frac{H_1}{2r}} \right) \left(e^{-i\frac{H_1}{2r}} \dots e^{-i\frac{H_L}{2r}} \right) \right]^r \text{ for Trotter2,} \quad (\text{B.7})$$

Table III. Experiment setting

Application	Benchmarking	TSP	TD-QDS	VQE
Cost function	$\mathcal{L}(2)$	$\mathcal{F}(7), \mathcal{F}_{\text{ws}}(\text{B.2})$	$\mathcal{L}^2(\text{B.9})$	$\mathcal{L}_{\text{VQE}}(11)$
Evaluated object	Haar random unitary	Thermal state	Heisenberg models	H ₂ molecules
Optimizer	Adam	Adam	Adam	COBYLA
N	[2 – 5]	[2-8]	2	4
	$d = [2 - 39]$	$d = 2N$	$d = 4$	$d = [15, 18, 20, 24, 25]$
Hyper-parameter	$n_{\mathcal{V}} = [4, 8, 16, 32]$	$n_{\mathcal{V}} = 8$	$n_{\mathcal{V}} = 8$	$n_{\mathcal{V}} = 8$
	$n_{\text{gene}} = [10, 20, 30, 40]$	$n_{\text{gene}} = 16$	$n_{\text{gene}} = 16$	$n_{\text{gene}} = 20$

where r is the Trotter number. In this work, we set $r = 100$.

c. AVQDS method.

The AVQDS method, introduced in Ref. [8], works as follows. Starting with the initial quantum state $|\psi_0\rangle$, the state evolves over time according to $|\psi(t)\rangle$ as

$$\frac{d|\psi(t)\rangle}{dt} = -iH(t)|\psi(t)\rangle. \quad (\text{B.8})$$

To solve this, we use a variational quantum ansatz $|\psi(\boldsymbol{\theta}(t))\rangle$, where $\boldsymbol{\theta}(t)$ represents a set of time-dependent parameters. For example, at time $t = 0$, it gives $|\psi(\boldsymbol{\theta}(t = 0))\rangle = |\psi_0\rangle$. These parameters are trained to minimize the squared McLachlan distance [61] \mathcal{L}^2

$$\mathcal{L}^2 = \left\| \sum_{\mu} \frac{d|\psi(\boldsymbol{\theta})\rangle}{d\theta_{\mu}} \frac{d\theta_{\mu}}{dt} + iH(t)|\psi(\boldsymbol{\theta})\rangle \right\|_F^2, \quad (\text{B.9})$$

where $\|\cdot\|_F$ denotes the Frobenius norm, and we omit t in $\boldsymbol{\theta}(t)$ to simplify the notation.

In our numerical simulation, we first construct the Hamiltonian $H(t)$ as described in Eq. (8). We then employ the pseudo-Trotter ansatz [8] $|\psi(\boldsymbol{\theta})\rangle = \prod_{\mu=1}^{N_{\boldsymbol{\theta}}} e^{-i\theta_{\mu}A_{\mu}}|\psi_0\rangle$, where $N_{\boldsymbol{\theta}}$ is the number of trainable

time-dependent parameters, and A_{μ} are Hermitian operators from a set of Pauli operators. During the simulation for any time $0 < t_i < T$, the ansatz is adaptively updated until the squared McLachlan distance meets the threshold $\mathcal{L}_{\text{cut}}^2$. We set the threshold $\mathcal{L}_{\text{cut}}^2 = 10^{-3}$ for Figure 4(a), and $\mathcal{L}_{\text{cut}}^2 = 10^{-1}$ for Figure 4(b,c). In Figure 4(b,c), the AVQDS method is not trainable at $\mathcal{L}_{\text{cut}}^2 = 10^{-3}$, so we temporarily reduce its accuracy by training at $\mathcal{L}_{\text{cut}}^2 = 10^{-1}$. This is why the accuracy of this method is lower compared to the exact result and GA-VQA method.

4. Variational quantum eigensolver

For the variational quantum eigensolver [56, 62], an upper bound of ground state energy E_o of a given Hamiltonian is bounded by

$$E_o \leq \frac{\langle \psi(\boldsymbol{\theta}) | H | \psi(\boldsymbol{\theta}) \rangle}{\langle \psi(\boldsymbol{\theta}) | \psi(\boldsymbol{\theta}) \rangle} \equiv \langle H \rangle, \quad (\text{B.10})$$

which is found by optimizing the parameters of quantum state $|\psi\rangle \equiv V_l(\boldsymbol{\theta})|\mathbf{0}\rangle$. To simulate the GA-VQA scheme's application in VQE with a Hydrogen molecule, we run GA-VQA with the setup that can be seen in the VQE field at Tab. III. In this case, the target of the GA-VQA is to find ansatzes with low depth but still gain the needed accuracy of ground state molecular energy. The GA is leveraged to find the friendly NISQ ansatz while the optimizing part is left to VQE. This method iteratively converges to higher fidelity (the higher the fidelity, the more accurate the result) until the max generation or termination condition is satisfied.

[1] M. Cerezo, Andrew Arrasmith, Ryan Babbush, Simon C. Benjamin, Suguru Endo, Keisuke Fujii, Jarrod R. McClean, Kosuke Mitarai, Xiao Yuan, Lukasz Cincio, and Patrick J. Coles. Variational quantum algorithms. *Nature Reviews Physics*, 3(9):625–644, Sep 2021.

[2] Viacheslav V. Kuzmin and Pietro Silvi. Variational quantum state preparation via quantum data buses. *Quantum*, 4:290, July 2020.

[3] R. Sagastizabal, S. P. Premaratne, B. A. Klaver, M. A. Rol, V. Negirneac, M. S. Moreira, X. Zou, S. Johri, N. Muthusubramanian, M. Beekman, C. Zachariadis, V. P. Ostroukh, N. Haider, A. Bruno, A. Y. Matsuura, and L. DiCarlo. Variational preparation of finite-temperature states on a quantum computer. *npj Quantum Information*, 7(1):130, Aug 2021.

[4] Xiao-Ming Zhang, Tongyang Li, and Xiao Yuan. Quantum state preparation with optimal circuit depth: Im-

- plementations and applications. *Phys. Rev. Lett.*, 129:230504, Nov 2022.
- [5] Juan C. Zuñiga Castro, Jeffrey Larson, Sri Hari Krishna Narayanan, Victor E. Colussi, Michael A. Perlin, and Robert J. Lewis-Swan. Variational quantum state preparation for quantum-enhanced metrology in noisy systems, 2024.
- [6] Vu Tuan Hai, Nguyen Tan Viet, and Le Bin Ho. Variational preparation of entangled states on quantum computers. *arXiv preprint arXiv:2306.17422*, 2023.
- [7] Vu Tuan Hai, Nguyen Tan Viet, and Le Bin Ho. <code>qoqop</code>: A quantum object optimizer. *SoftwareX*, 26:101726, 2024.
- [8] Yong-Xin Yao, Niladri Gomes, Feng Zhang, Cai-Zhuang Wang, Kai-Ming Ho, Thomas Iadecola, and Peter P. Orth. Adaptive variational quantum dynamics simulations. *PRX Quantum*, 2:030307, Jul 2021.
- [9] Jianming Luo, Kaihan Lin, and Xing Gao. Variational quantum simulation of lindblad dynamics via quantum state diffusion. *The Journal of Physical Chemistry Letters*, 15(13):3516–3522, Apr 2024.
- [10] David Linteau, Stefano Barison, Netanel H. Lindner, and Giuseppe Carleo. Adaptive projected variational quantum dynamics. *Phys. Rev. Res.*, 6:023130, May 2024.
- [11] Bálint Koczor, Suguru Endo, Tyson Jones, Yuichiro Matsuzaki, and Simon C Benjamin. Variational-state quantum metrology. *New Journal of Physics*, 22(8):083038, aug 2020.
- [12] Ziqi Ma, Pranav Gokhale, Tian-Xing Zheng, Sisi Zhou, Xiaofei Yu, Liang Jiang, Peter Maurer, and Frederic T. Chong. Adaptive circuit learning for quantum metrology. In *2021 IEEE International Conference on Quantum Computing and Engineering (QCE)*, pages 419–430, 2021.
- [13] Johannes Jakob Meyer, Johannes Borregaard, and Jens Eisert. A variational toolbox for quantum multiparameter estimation. *npj Quantum Information*, 7(1):89, Jun 2021.
- [14] Trung Kien Le, Hung Q. Nguyen, and Le Bin Ho. Variational quantum metrology for multiparameter estimation under dephasing noise. *Scientific Reports*, 13(1):17775, Oct 2023.
- [15] Valeria Cimini, Mauro Valeri, Simone Piacentini, Francesco Ceccarelli, Giacomo Corrielli, Roberto Oselame, Nicolò Spagnolo, and Fabio Sciarrino. Variational quantum algorithm for experimental photonic multiparameter estimation. *npj Quantum Information*, 10(1):26, Feb 2024.
- [16] Zhiyan Ding, Xiantao Li, and Lin Lin. Simulating open quantum systems using hamiltonian simulations. *PRX Quantum*, 5:020332, May 2024.
- [17] Kentaro Heya, Yasunari Suzuki, Yasunobu Nakamura, and Keisuke Fujii. Variational quantum gate optimization, 2018.
- [18] Sumeet Khatri, Ryan LaRose, Alexander Poremba, Lukasz Cincio, Andrew T. Sornborger, and Patrick J. Coles. Quantum-assisted quantum compiling. *Quantum*, 3:140, May 2019.
- [19] Tyler Volkoff, Zoé Holmes, and Andrew Sornborger. Universal compiling and (no-)free-lunch theorems for continuous-variable quantum learning. *PRX Quantum*, 2:040327, Nov 2021.
- [20] Vu Tuan Hai and Le Bin Ho. Universal compilation for quantum state tomography. *Scientific Reports*, 13(1):3750, Mar 2023.
- [21] Mária Kieferová, Artur Scherer, and Dominic W. Berry. Simulating the dynamics of time-dependent hamiltonians with a truncated dyson series. *Phys. Rev. A*, 99:042314, Apr 2019.
- [22] Dominic W. Berry and Pedro C. S. Costa. Quantum algorithm for time-dependent differential equations using Dyson series. *Quantum*, 8:1369, June 2024.
- [23] Kaoru Mizuta and Keisuke Fujii. Optimal Hamiltonian simulation for time-periodic systems. *Quantum*, 7:962, March 2023.
- [24] Jingxiang Wu and Timothy H. Hsieh. Variational thermal quantum simulation via thermofield double states. *Phys. Rev. Lett.*, 123:220502, Nov 2019.
- [25] D. Zhu, S. Johri, N. M. Linke, K. A. Landsman, C. Huerta Alderete, N. H. Nguyen, A. Y. Matsuura, T. H. Hsieh, and C. Monroe. Generation of thermofield double states and critical ground states with a quantum computer. *Proceedings of the National Academy of Sciences*, 117(41):25402–25406, September 2020.
- [26] Youle Wang, Guangxi Li, and Xin Wang. Variational quantum gibbs state preparation with a truncated taylor series. *Phys. Rev. Appl.*, 16:054035, Nov 2021.
- [27] Brandon S. Harms, Blake E. Anthony, Noah T. Holte, Hunter A. Dassonville, and Andrew M. C. Dawes. Multimode quantum state tomography using unbalanced array detection. *Phys. Rev. A*, 90:053818, Nov 2014.
- [28] Kevin He, Ming Yuan, Yat Wong, Srivatsan Chakram, Alireza Seif, Liang Jiang, and David I. Schuster. Efficient multimode wigner tomography. *Nature Communications*, 15(1):4138, May 2024.
- [29] Tatsuhiko N. Ikeda, Asir Abrar, Isaac L. Chuang, and Sho Sugiura. Minimum Trotterization Formulas for a Time-Dependent Hamiltonian. *Quantum*, 7:1168, November 2023.
- [30] Tatsuhiko N. Ikeda, Hideki Kono, and Keisuke Fujii. Trotter24: A precision-guaranteed adaptive stepsize trotterization for hamiltonian simulations, 2023.
- [31] Yuxuan Du, Tao Huang, Shan You, Min-Hsiu Hsieh, and Dacheng Tao. Quantum circuit architecture search for variational quantum algorithms. *npj Quantum Information*, 8(1):62, May 2022.
- [32] Shi-Xin Zhang, Chang-Yu Hsieh, Shengyu Zhang, and Hong Yao. Neural predictor based quantum architecture search. *Machine Learning: Science and Technology*, 2(4):045027, oct 2021.
- [33] Li Li, Minjie Fan, Marc Coram, Patrick Riley, and Stefan Leichenauer. Quantum optimization with a novel gibbs objective function and ansatz architecture search. *Phys. Rev. Res.*, 2:023074, Apr 2020.
- [34] Zhimin He, Chuangtao Chen, Lvzhou Li, Shenggen Zheng, and Haozhen Situ. Quantum architecture search with meta-learning. *Advanced Quantum Technologies*, 5(8):2100134, 2022.
- [35] Harper R. Grimsley, Sophia E. Economou, Edwin Barnes, and Nicholas J. Mayhall. An adaptive variational algorithm for exact molecular simulations on a quantum computer. *Nature Communications*, 10(1):3007, Jul 2019.
- [36] B.I.P. Rubinstein. Evolving quantum circuits using genetic programming. In *Proceedings of the 2001 Congress on Evolutionary Computation (IEEE Cat. No.01TH8546)*, volume 1, pages 144–151 vol. 1, 2001.

- [37] Annu Lambora, Kunal Gupta, and Kriti Chopra. Genetic algorithm- a literature review. In 2019 International Conference on Machine Learning, Big Data, Cloud and Parallel Computing (COMITCon), pages 380–384, 2019.
- [38] Sourabh Katoch, Sumit Singh Chauhan, and Vijay Kumar. A review on genetic algorithm: past, present, and future. Multimedia Tools and Applications, 80(5):8091–8126, Feb 2021.
- [39] Daniel Tandeitnik and Thiago Guerreiro. Evolving quantum circuits. Quantum Information Processing, 23(3), March 2024.
- [40] Mateusz Ostaszewski, Edward Grant, and Marcello Benedetti. Structure optimization for parameterized quantum circuits. Quantum, 5:391, January 2021.
- [41] Ang Li and et al. Qasmbench: A low-level quantum benchmark suite for nisq evaluation and simulation. ACM Transactions on Quantum Computing, 4(2), feb 2023.
- [42] Floyd M. Creevey, Charles D. Hill, and Lloyd C. L. Hollenberg. Gasp: a genetic algorithm for state preparation on quantum computers. Scientific Reports, 13(1):11956, Jul 2023.
- [43] Sahel Ashhab, Naoki Yamamoto, Fumiki Yoshihara, and Kouichi Semba. Numerical analysis of quantum circuits for state preparation and unitary operator synthesis. Phys. Rev. A, 106:022426, Aug 2022.
- [44] Sahel Ashhab, Fumiki Yoshihara, Miwako Tsuji, Mitsuhiro Sato, and Kouichi Semba. Quantum circuit synthesis via a random combinatorial search. Phys. Rev. A, 109:052605, May 2024.
- [45] Matthias C. Caro, Hsin-Yuan Huang, Nicholas Ezzell, Joe Gibbs, Andrew T. Sornborger, Lukasz Cincio, Patrick J. Coles, and Zoë Holmes. Out-of-distribution generalization for learning quantum dynamics. Nature Communications, 14(1):3751, Jul 2023.
- [46] Nic Ezzell, Elliott M Ball, Aliza U Siddiqui, Mark M Wilde, Andrew T Sornborger, Patrick J Coles, and Zoë Holmes. Quantum mixed state compiling. Quantum Science and Technology, 8(3):035001, 2023.
- [47] Jacob M. Leamer, Wenlei Zhang, Ravi K. Saripalli, Ryan T. Glasser, and Denys I. Bondar. Simulation of quantum gibbs states using epsilon-near-zero materials and classical light. In Conference on Lasers and Electro-Optics, page JTU3A.72. Optica Publishing Group, 2021.
- [48] Mohammad H. Amin, Evgeny Andriyash, Jason Rolfe, Bohdan Kulchytskyy, and Roger Melko. Quantum boltzmann machine. Phys. Rev. X, 8:021050, May 2018.
- [49] Luuk Coopmans, Yuta Kikuchi, and Marcello Benedetti. Predicting gibbs-state expectation values with pure thermal shadows. PRX Quantum, 4:010305, Jan 2023.
- [50] Mathieu Lewin, Phan Thành Nam, and Nicolas Rougerie. Classical field theory limit of many-body quantum gibbs states in 2d and 3d. Inventiones mathematicae, 224(2):315–444, May 2021.
- [51] W. Israel. Thermo-field dynamics of black holes. Physics Letters A, 57(2):107–110, 1976.
- [52] Ping Gao, Daniel Louis Jafferis, and Aron C. Wall. Traversable wormholes via a double trace deformation. Journal of High Energy Physics, 2017(12):151, Dec 2017.
- [53] Wen Wei Ho and Timothy H. Hsieh. Efficient variational simulation of non-trivial quantum states. SciPost Phys., 6:029, 2019.
- [54] Shavindra P. Premaratne and A. Y. Matsuura. Engineering a cost function for real-world implementation of a variational quantum algorithm. In 2020 IEEE International Conference on Quantum Computing and Engineering (QCE). IEEE, 10 2020.
- [55] Hongzheng Zhao, Marin Bukov, Markus Heyl, and Roderich Moessner. Adaptive trotterization for time-dependent hamiltonian quantum dynamics using instantaneous conservation laws, 2023.
- [56] Alberto Peruzzo, Jarrod McClean, Peter Shadbolt, Man-Hong Yung, Xiao-Qi Zhou, Peter J. Love, Alán Aspuru-Guzik, and Jeremy L. O’Brien. A variational eigenvalue solver on a photonic quantum processor. Nature Communications, 5(1):4213, Jul 2014.
- [57] Jonathan Romero, Ryan Babbush, Jarrod R McClean, Cornelius Hempel, Peter J Love, and Alán Aspuru-Guzik. Strategies for quantum computing molecular energies using the unitary coupled cluster ansatz. Quantum Science and Technology, 4(1):014008, oct 2018.
- [58] Daniel Gottesman. Theory of fault-tolerant quantum computation. Phys. Rev. A, 57:127–137, Jan 1998.
- [59] Vu Tuan Hai and Le Bin Ho. Lagrange Interpolation Approach for General Parameter-Shift Rule, pages 1–17. Springer International Publishing, Cham, 2024.
- [60] David Layden. First-order trotter error from a second-order perspective. Phys. Rev. Lett., 128:210501, May 2022.
- [61] A.D. McLachlan. A variational solution of the time-dependent schrodinger equation. Molecular Physics, 8(1):39–44, 1964.
- [62] Jules Tilly, Hongxiang Chen, Shuxiang Cao, Dario Picozzi, Kanav Setia, Ying Li, Edward Grant, Leonard Wossnig, Ivan Rungger, George H. Booth, and Jonathan Tennyson. The variational quantum eigensolver: A review of methods and best practices. Physics Reports, 986:1–128, 2022. The Variational Quantum Eigensolver: a review of methods and best practices.